

Supporting Information for

Reviving BVDT-TTF and EVT-TTF salts

Federica Solano,¹ Pascale Auban-Senzier,² Bolesław Barszcz³, Arkadiusz Frąckowiak³, Iwona Olejniczak³, Pere Alemany,⁴ Enric Canadell,^{*,5} Nicolas Zigon^{*1}, Narcis Avarvari^{*1}

¹ Univ Angers, CNRS, MOLTECH-ANJOU, SFR MATRIX, F-49000 Angers, France. E-mail: narcis.avarvari@univ-angers.fr; nicolas.zigon@univ-angers.fr

² Université Paris-Saclay, CNRS, UMR 8502, Laboratoire de Physique des Solides, 91405 Orsay, France

³ Institute of Molecular Physics, Polish Academy of Sciences, Smoluchowskiego 17, 60-179 Poznań, Poland

⁴ Departament de Ciència de Materials i Química Física and Institut de Química Teòrica i Computacional (IQTCUB), Universitat de Barcelona, Martí i Franquès 1, 08028 Barcelona, Spain

⁵ Institut de Ciència de Materials de Barcelona, ICMAB-CSIC, Campus de la UAB, 08193 Bellaterra, Spain, and Royal Academy of Sciences and Arts of Barcelona, Chemistry Section, La Rambla 115, 08002 Barcelona, Spain. E-mail: canadell@icmab.es

SUMMARY

Table S1. Crystallographic data, details of data collection and structure refinement parameters.

Table S2. Stoichiometry and conductivity of BVDT-TTF, EVT-TTF and BEDT-TTF salts.

Figure S1. Temperature dependent resistivity measurement on single crystal for $(\text{BVDT-TTF})_{2.5}(\text{I}_3)$.

Figure S2. Temperature dependent resistivity measurement on single crystal for $(\text{BVDT-TTF})_2(\text{ReO}_4)$.

Figure S3. Temperature dependent resistivity measurement on single crystal for $(\text{EVT-TTF})(\text{ClO}_4)$.

Figure S4. Raman spectrum of $(\text{BVDT-TTF})_{2.5}(\text{I}_3)$ measured at room temperature with the 632.8 nm excitation line, in the frequency range of the polyiodide stretching vibrations.

Figure S5. ^1H NMR (300 MHz, CDCl_3) of compound **3**.

Figure S6. ^3C NMR (76 MHz, CDCl_3) of compound **3**.

Figure S7. ^1H NMR (300 MHz, CDCl_3) of compound **4**.

Figure S8. ^3C NMR (76 MHz, CDCl_3) of compound **4**.

Figure S9. ^1H NMR (300 MHz, CDCl_3) of compound **BVDT-TTF**.

Figure S10. ^1H NMR (300 MHz, CDCl_3) of compound **EVT-TTF**.

Figure S11. ^{13}C NMR (126 MHz, DMSO-d_6) of compound **EVT-TTF**.

Figure S12. MS (MALDI-TOF) of compound **BVDT-TTF**.

Figure S13. MS (MALDI-TOF) of compound **4**.

Figure S14. MS (MALDI-TOF) of compound **EVT-TTF**.

Figure S15. MS (MALDI-TOF) of compound **3**.

Table S1 Crystallographic data, details of data collection and structure refinement parameters.

	(BVDT-TTF)(TaF₆)	(BVDT-TTF)_{2.5}(I₃)	(BVDT-TTF)₂(ReO₄)	(EVT-TTF)(ClO₄)
Formula sum	C ₁₀ H ₄ S ₈ , TaF ₆	C ₁₀ H ₄ S ₈ , I _{1.2}	C ₁₀ H ₄ S ₈ , (ClO ₄) _{0.5}	C ₁₀ H ₆ S ₈ , (CH ₂ Cl ₂) _{0.5} , ClO ₄
Formula weight	675.56	532.89	505.71	524.54
Crystal system	orthorhombic	orthorhombic	monoclinic	monoclinic
Space group	Pnnm	Pnma	C2/m	P2 ₁ /c
a/Å	4.8259(3)	3.777(19)	33.133(3)	8.0005(4)
b/Å	17.8935(9)	12.18(14)	12.1739(14)	23.8718(10)
c/Å	10.1805(5)	33.1(9)	3.8263(6)	9.8100(5)
α/°	90	90	90	90
β/°	90	90	93.360(11)	100.649(5)
γ/°	90	90	90	90
V/Å ³	879.11(8)	1523(46)	1540.7(3)	1841.31(16)
Z	2	4	4	4
D _c /g cm ⁻³	2.552	2.324	2.180	1.892
T/K	200	200	200	297
μ/mm ⁻¹	20.964	29.814	18.139	11.819
Reflections collected	883	1518	1714	6003
Independent reflection	826	1207	1035	2614
final R ₁ ^a , wR ₂ ^b [I > 2σ(I)]	0.0393/0.1129	0.0795/0.2430	0.1192/0.3454	0.0570/0.1564
R ₁ ^a ,wR ₂ ^b (all data)	0.0408/0.1141	0.0943/0.2540	0.1249/0.3489	0.0646/0.1653
goodness-of-fit on F ²	1.099	1.131	1.097	1.055
Δρ _{min} /Δρ _{max} (e Å ⁻³)	-1.305/2.169	-0.755/1.261	-0.971/1.102	-0.938/0.984
Completeness (%)	99.2	98.4	81.0	94.1
CCDC number	2296888-	2296889-	2296890-	2296891-

^aR₁ = Σ||F_o| - |F_c|| / Σ|F_o|. ^bwR₂ = [Σw(F_o² - F_c²)² / Σw(F_o²)²]^{1/2}; w = 1/[σ²(F_o²) + (aP)² + bP] where P = [max(F_o², 0) + 2F_c²]/3.

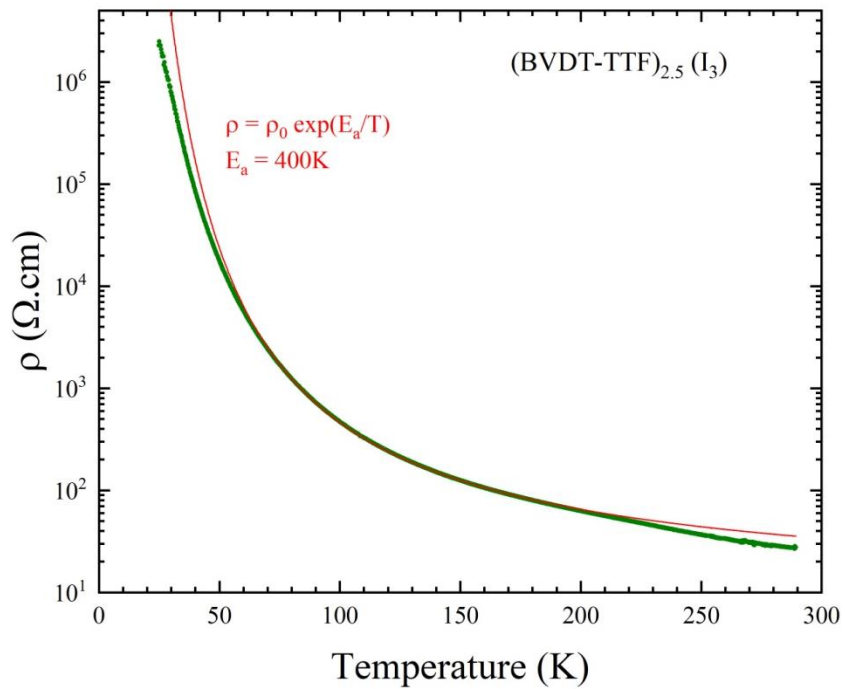


Fig. S1 Temperature dependent resistivity measurement on single crystal for (BVDT-TTF)_{2.5}(I₃).

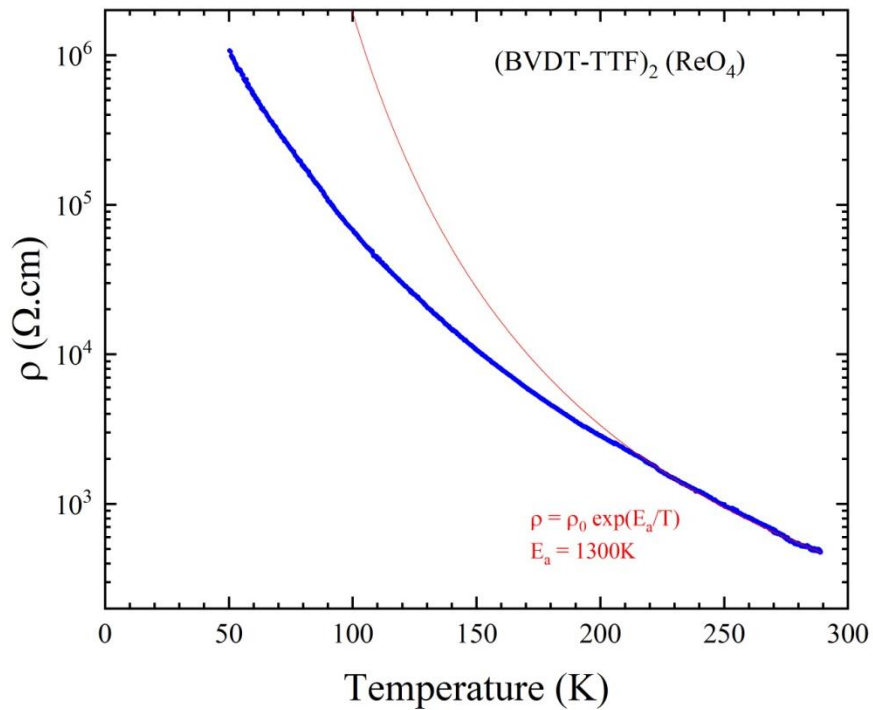


Fig. S2 Temperature dependent resistivity measurement on single crystal for (BVDT-TTF)₂(ReO₄).

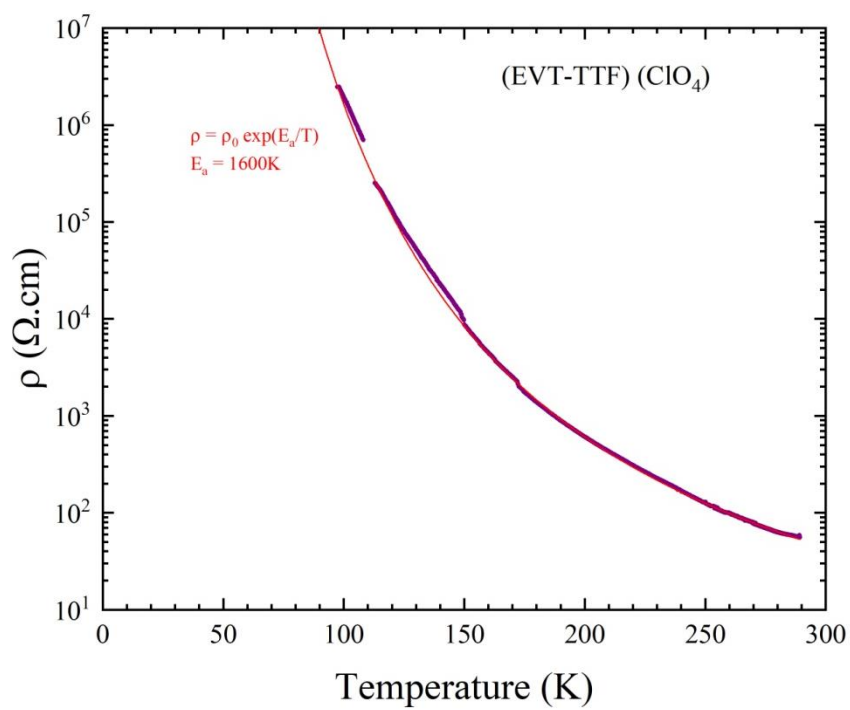


Fig. S3 Temperature dependent resistivity measurement on single crystal for (EVT-TTF)(ClO_4).

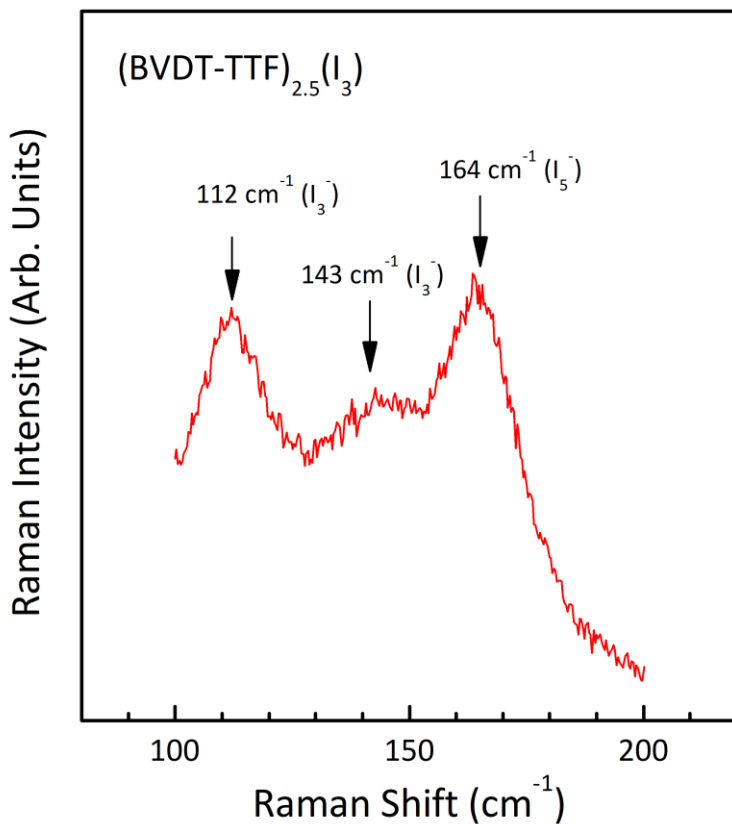


Fig. S4 Raman spectrum of $(\text{BVDT-TTF})_{2.5}(\text{I}_3)$ measured at room temperature with the 632.8 nm excitation line, in the frequency range of the polyiodide stretching vibrations.

The Raman spectrum of $(\text{BVDT-TTF})_{2.5}(\text{I}_3)$ in the frequency range of the stretching polyiodide modes reveals three distinct modes:

- the symmetric stretching of the centrosymmetric triiodide anion at 112 cm^{-1} ,
- the asymmetric stretching mode of the asymmetric triiodide ion at 143 cm^{-1} ,
- the band at 164 cm^{-1} , which is most likely related to the symmetric stretching of the L-shaped pentaiodide present in the structure.^{1,2}

Table S2 Stoichiometry and conductivity of BVDT-TTF, EVT-TTF and BEDT-TTF salts.

Donor	Anion	Stoichiometry	Single crystal conductivity (S·cm ⁻¹ , 290K)
BVDT-TTF	TaF ₆ ⁻	1 : 1	4.4·10 ⁻²
BVDT-TTF	I ₃ ⁻	2.5 : 1	1.4·10 ⁻¹
BVDT-TTF	ReO ₄ ⁻	2 : 1	3.1·10 ⁻³
EVT-TTF	ClO ₄ ⁻	1 : 1	1.8·10 ⁻²
BEDT-TTF ³	TaF ₆ ⁻	1 : 1	5·10 ⁻⁴
β -BEDT-TTF ⁴	I ₃ ⁻	2 : 1	20
BEDT-TTF ⁵	ReO ₄ ⁻	2 : 1	5·10 ⁻³
BEDT-TTF ⁶	ClO ₄ ⁻	2 : 1	26.31

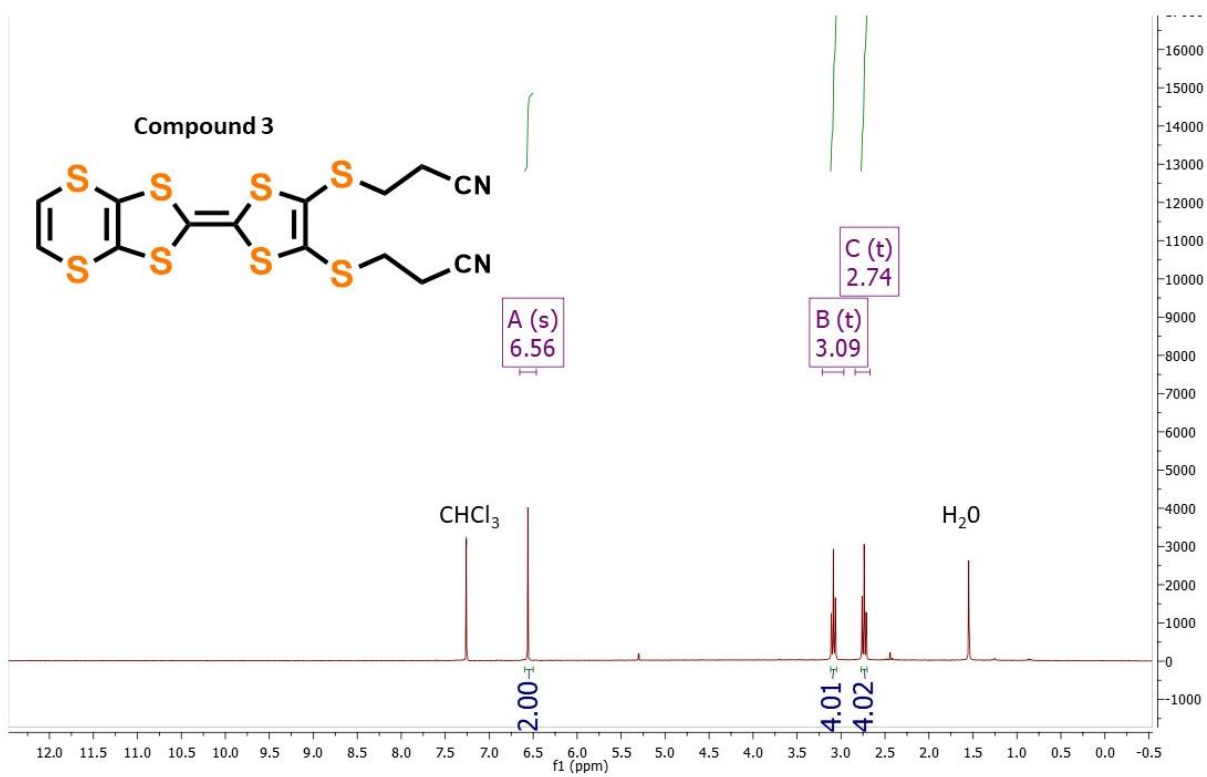


Fig. S5 ^1H NMR (300 MHz, CDCl₃) of compound **3**.

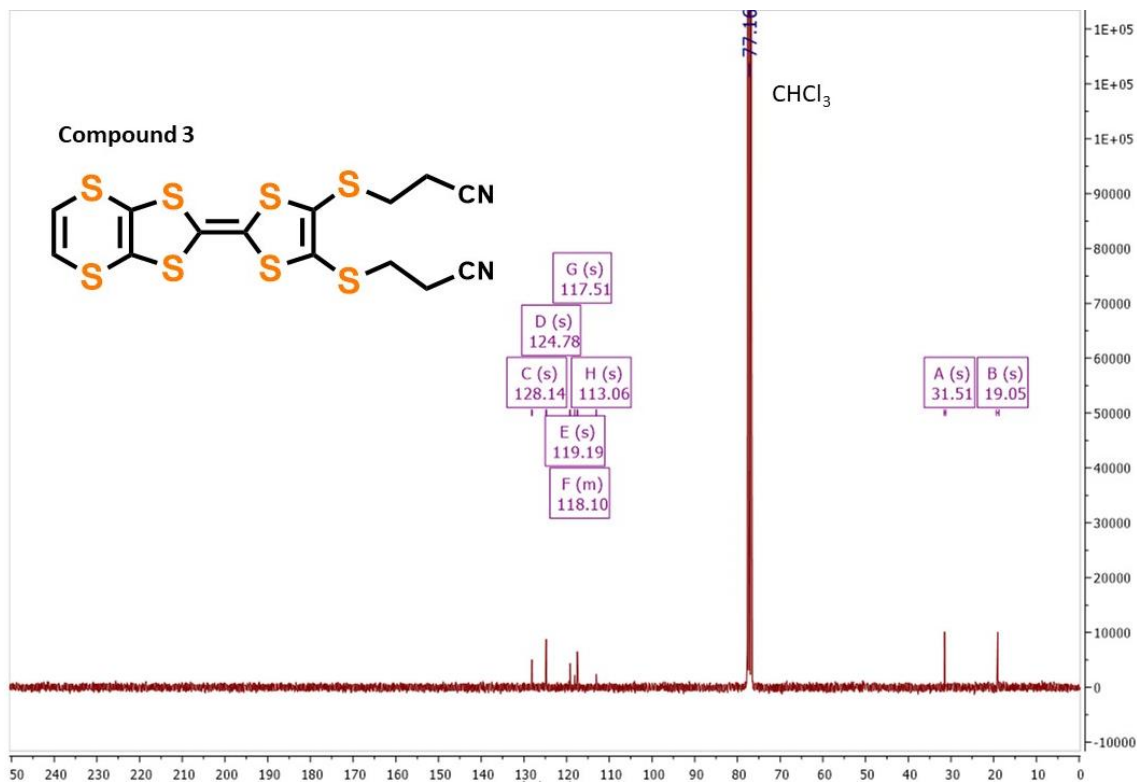


Fig. S6 ^{13}C NMR (76 MHz, CDCl₃) of compound **3**.

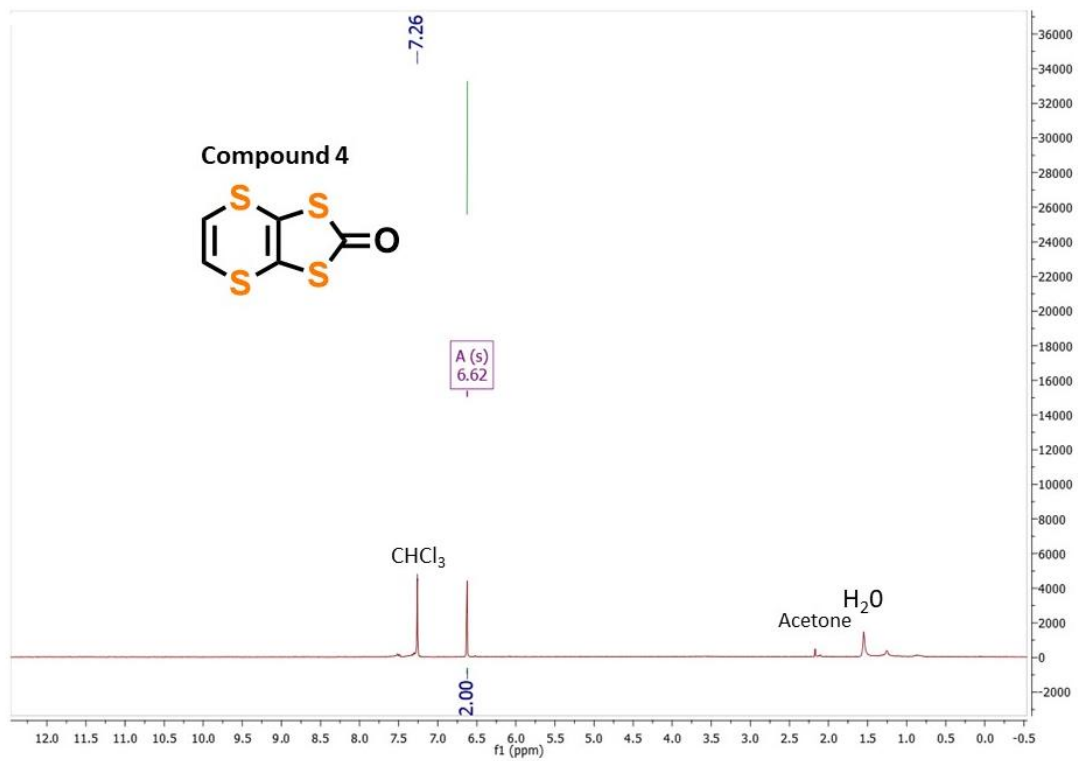


Fig. S7 ^1H NMR (300 MHz, CDCl_3) of compound 4.

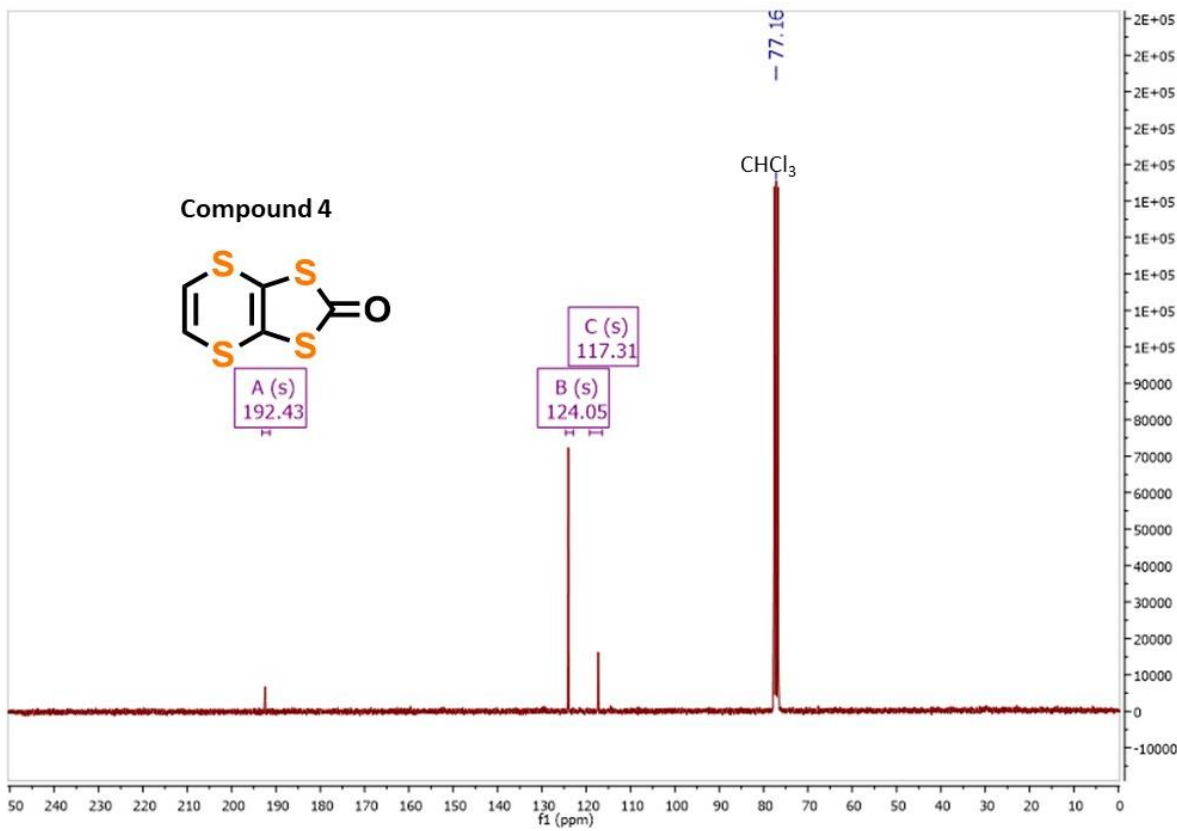


Fig. S8 ^{13}C NMR (76 MHz, CDCl_3) of compound 4.

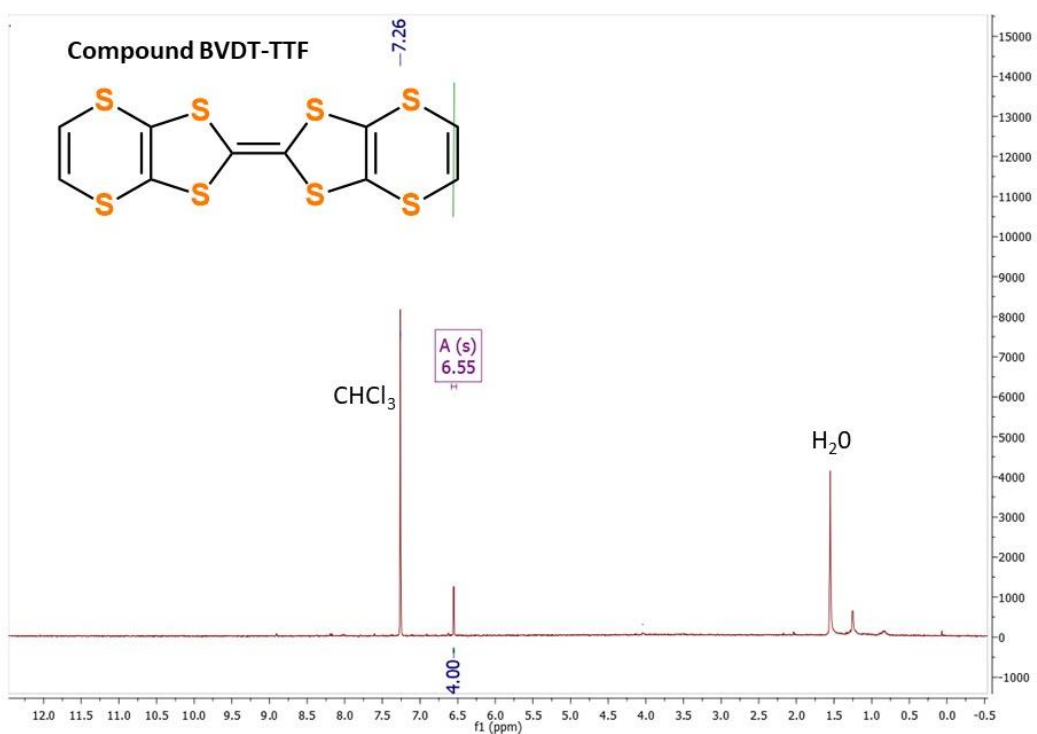


Fig. S9 ^1H NMR (300 MHz, CDCl_3) of **BVDT-TTF**.

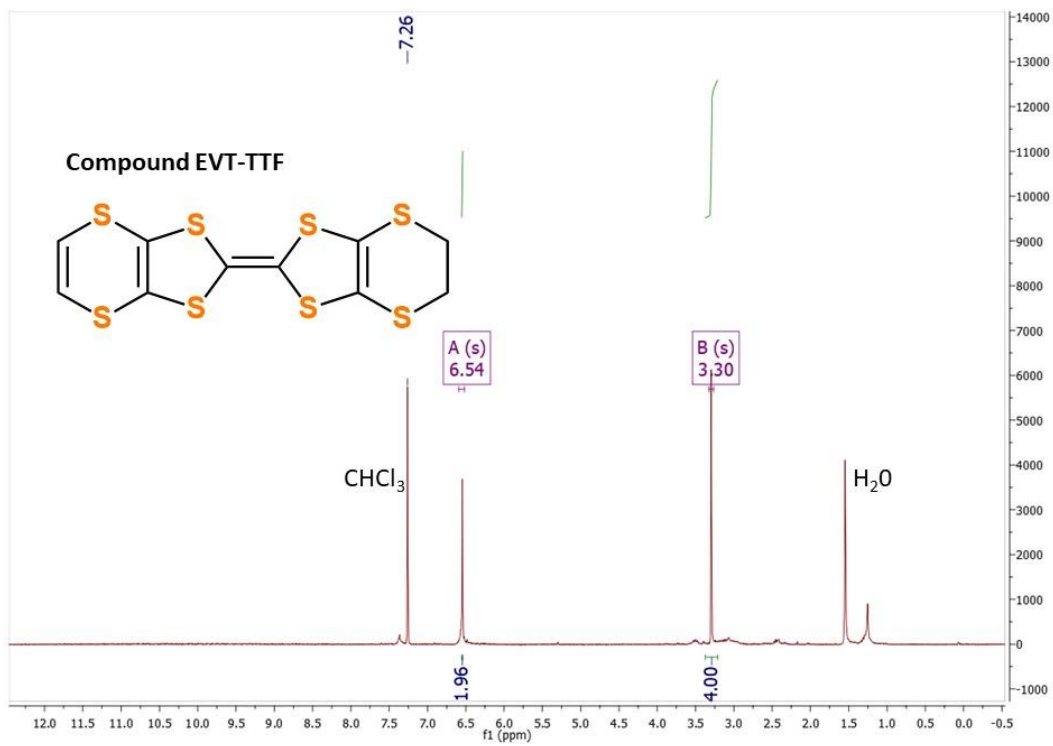


Fig. S10 ^1H NMR (300 MHz, CDCl_3) of **EVT-TTF**.

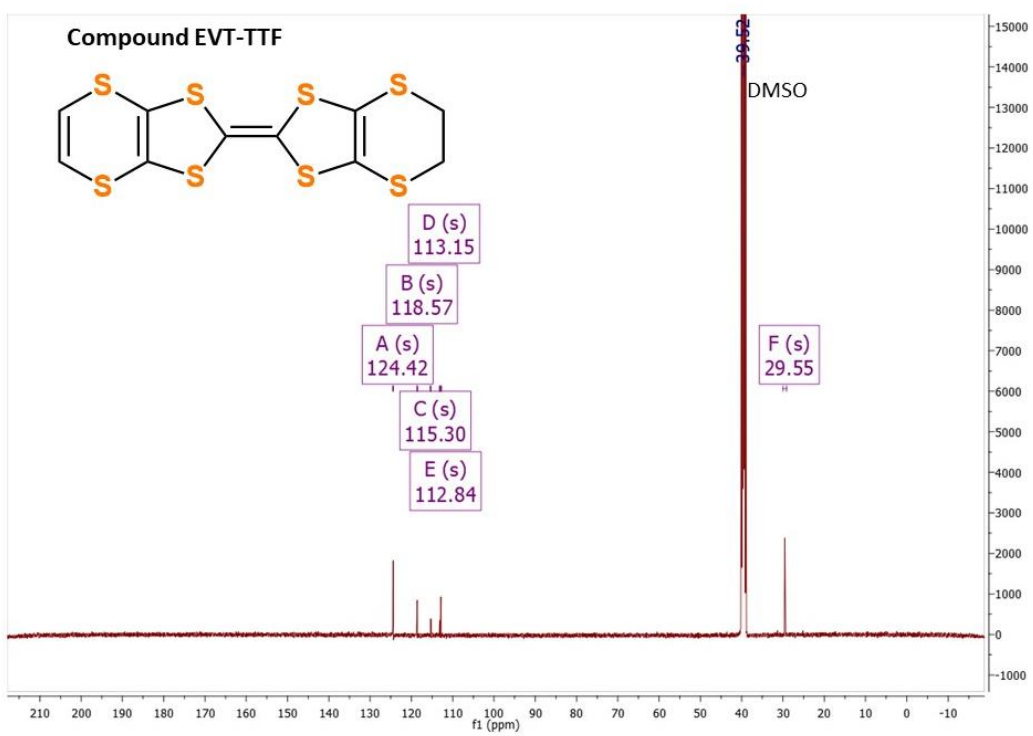


Fig. S11 ^{13}C NMR (126 MHz, DMSO-d_6) of EVT-TTF.

Mass spectrum:

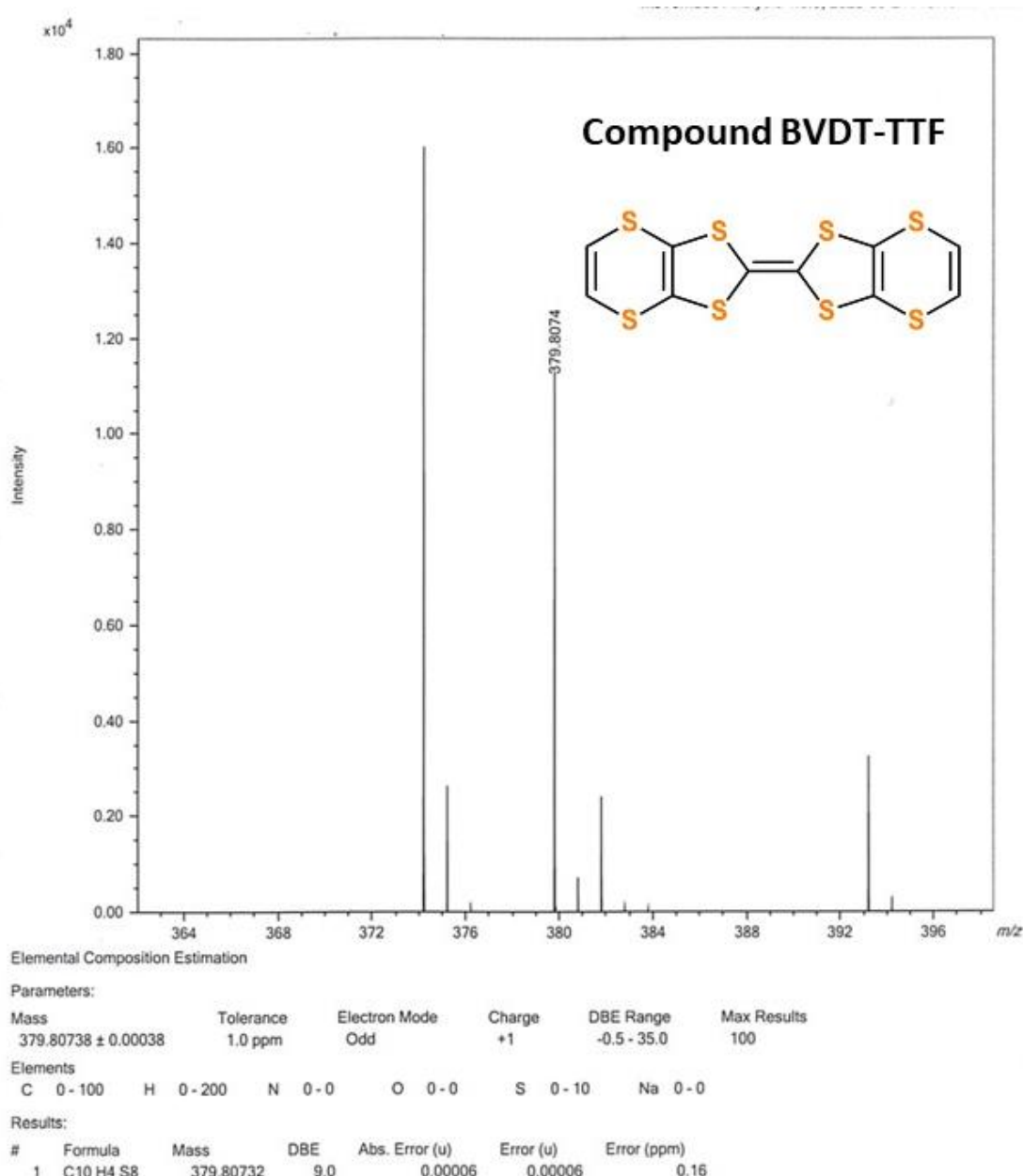


Fig. S12 MS (MALDI-TOF) of **BVDT-TTF**.

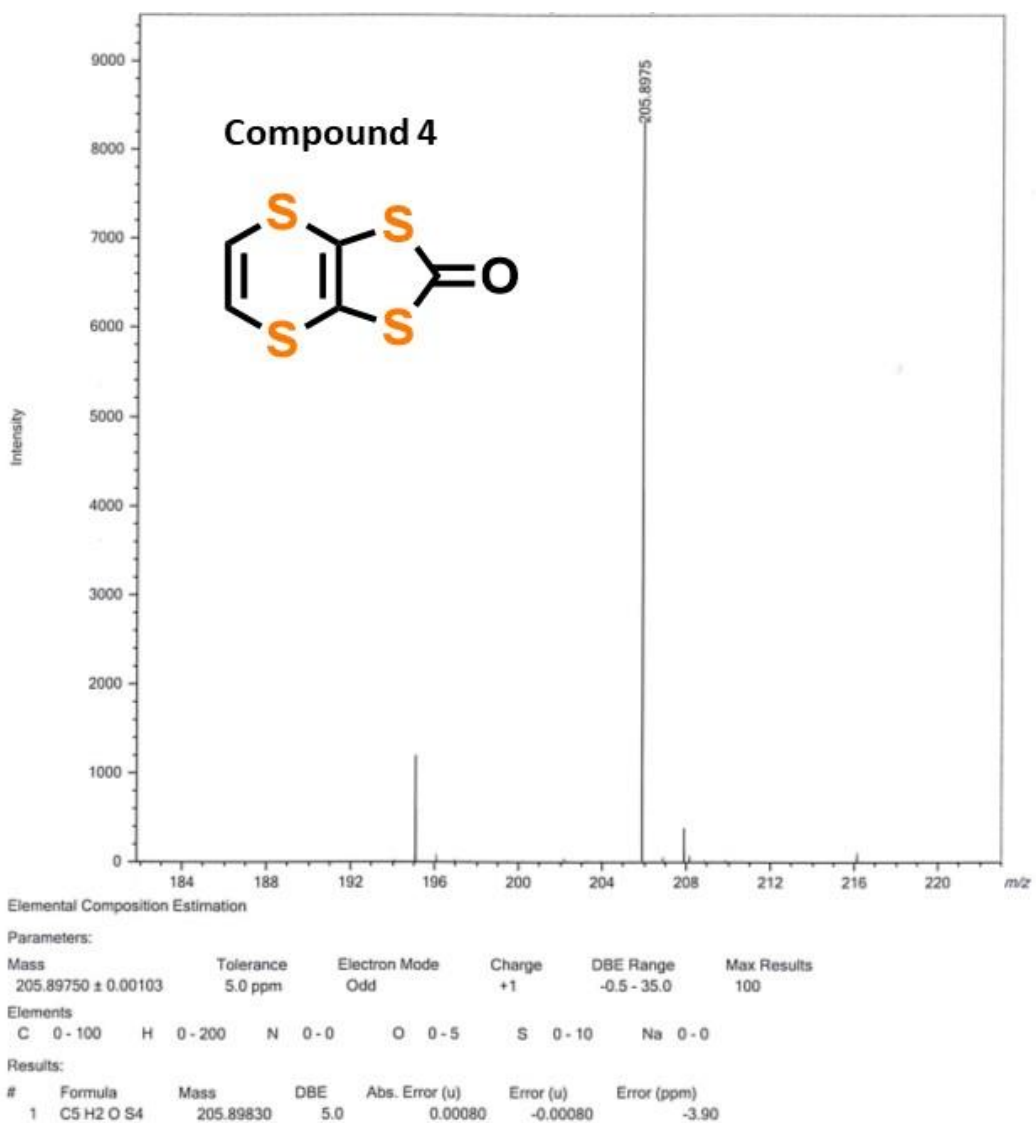


Fig. S13 MS (MALDI-TOF) of compound 4.

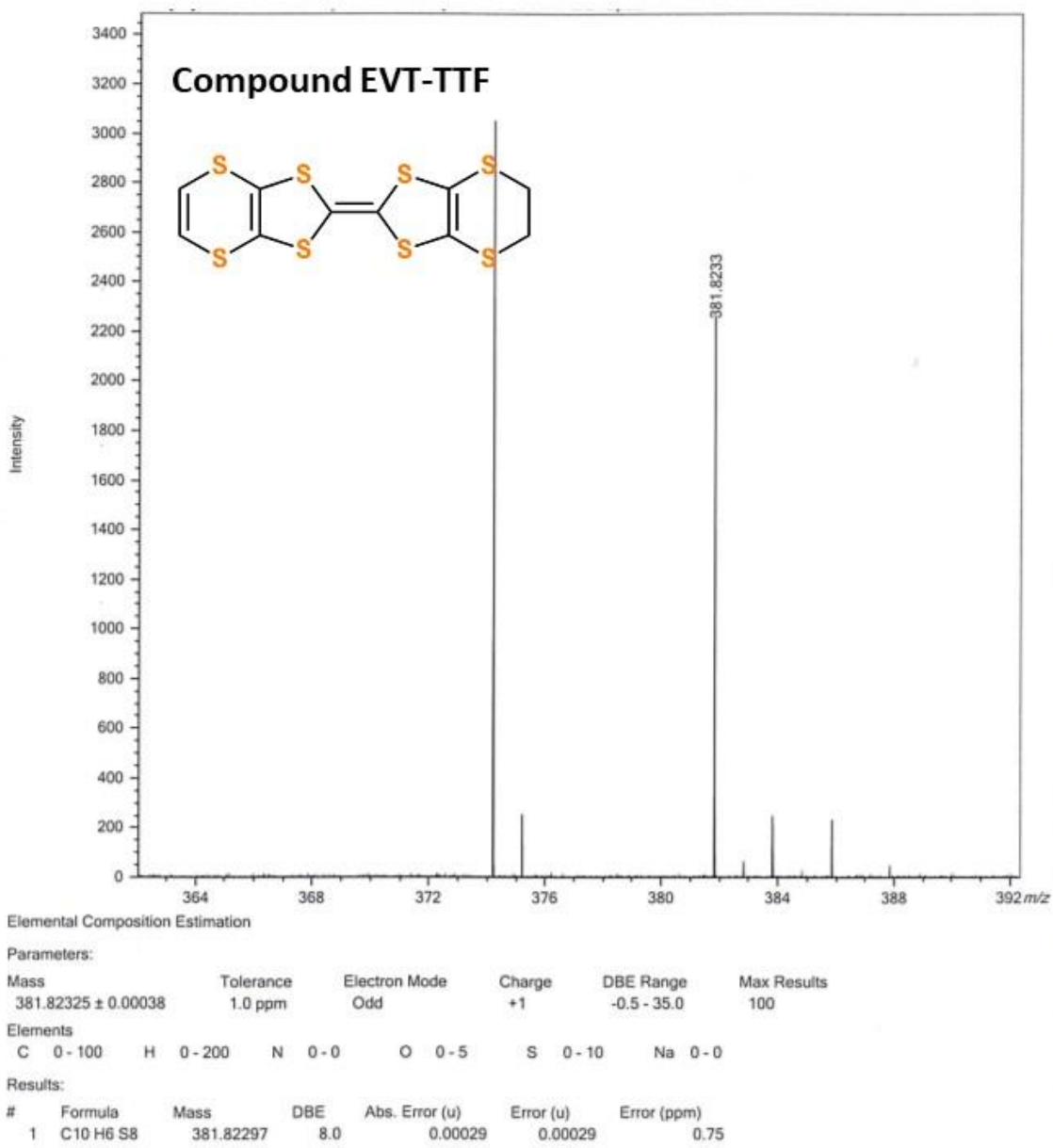


Fig. S14 MS (MALDI-TOF) of EVT-TTF.

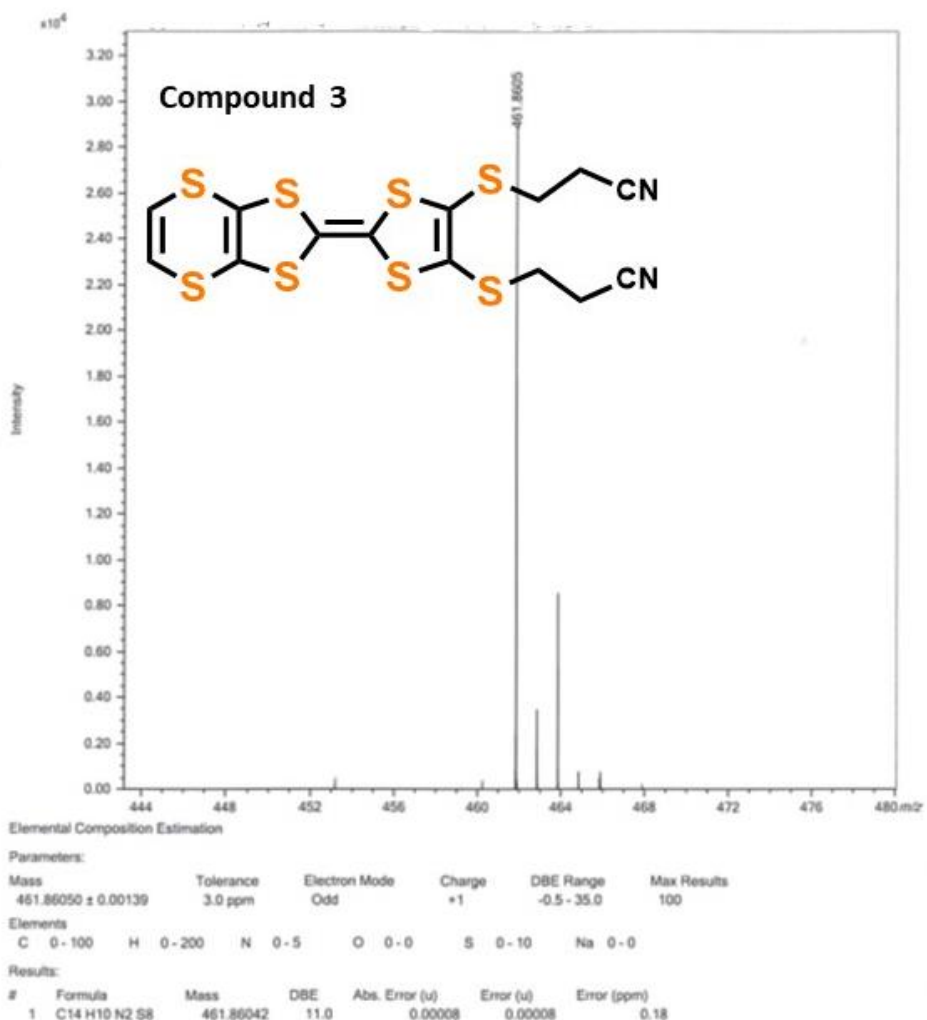


Fig. S15 MS (MALDI-TOF) of compound 3.

References

- 1 P. H. Svensson and L. Kloo, *Chem. Rev.*, 2003, **103**, 1649–1684.
- 2 I. Jerman, V. Jovanovski, A. Šurca Vuk, S. B. Hočevar, M. Gaberšček, A. Jesih and B. Orel, *Electrochim Acta*, 2008, **53**, 2281–2288.
- 3 M. Allain, C. Mézière, P. Auban-Senzier and N. Avarvari, *Crystals*, 2021, **11**, 386.
- 4 L. I. Buravov, M. V. Kartsovnik, V. F. Kaminskii, P. A. Kononovich, E. E. Kostuchenko, V. N. Laukhin, M. K. Makova, S. I. Pesotskii, V. N. Topnikov and E. B. Yagubskii, .
- 5 S. S. P. Parkin, E. M. Engler, R. R. Schumaker, R. Lagier, V. Y. Lee, J. C. Scott and R. L. Greene, *Phys. Rev. Lett.*, 1983, **50**, 270–273.
- 6 G. Saito, T. Enoki, K. Toriumi and H. Inokuchi, *Solid State Commun.*, 1982, **42**, 557–560.